

University of Nebraska - Lincoln

DigitalCommons@University of Nebraska - Lincoln

Peter Dowben Publications

Research Papers in Physics and Astronomy

10-2009

Isomeric effects with di-iodobenzene ($C_6H_4I_2$) on adsorption on graphite

Keisuke Fukutani

University of Nebraska-Lincoln

Ning Wu

University of Nebraska-Lincoln

Peter A. Dowben

University of Nebraska-Lincoln, pdowben@unl.edu

Follow this and additional works at: <https://digitalcommons.unl.edu/physicsdowben>

 Part of the [Physics Commons](#)

Fukutani, Keisuke; Wu, Ning; and Dowben, Peter A., "Isomeric effects with di-iodobenzene ($C_6H_4I_2$) on adsorption on graphite" (2009). *Peter Dowben Publications*. 236.

<https://digitalcommons.unl.edu/physicsdowben/236>

This Article is brought to you for free and open access by the Research Papers in Physics and Astronomy at DigitalCommons@University of Nebraska - Lincoln. It has been accepted for inclusion in Peter Dowben Publications by an authorized administrator of DigitalCommons@University of Nebraska - Lincoln.

Isomeric effects with di-iodobenzene (C₆H₄I₂) on adsorption on graphite

Keisuke Fukutani, Ning Wu, and P. A. Dowben

Department of Physics and Astronomy, Nebraska Center for Materials and Nanoscience,
University of Nebraska–Lincoln, Lincoln, NE 68588-0111, USA

Corresponding author – Peter A. Dowben, tel 402 472-9838, fax 402 472-2879, email pdowben@unl.edu

Abstract

Differences are seen in the adsorption of 1,2-di-iodobenzene, 1,3-di-iodobenzene, and 1,4-di-iodobenzene on graphite, as a function of exposure, using core level photoemission. The isomer 1,3-di-iodobenzene exhibits significant differences from 1,2-di-iodobenzene, and 1,4-di-iodobenzene in apparent sticking coefficients and core level binding energies. 1,3-Di-iodobenzene adsorb on graphite at 110 K in a strongly Stranski–Krastanov or Volmer–Weber (island) growth mode. The implication is that, even for small molecules adsorption, the adsorbate dipole in the plane of surface and the choice of isomer may matter.

Keywords: halocarbon adsorption, halobenzenes, dipole interactions, adsorption kinetics

1. Introduction

For many large molecule adlayers, including a number of organic and metal–organic species, the energy level alignment of the adsorbate with respect to a conducting substrate Fermi level or adjacent layer chemical potential is dependent on the interfacial electronic structure and interfacial dipole layer, as has been demonstrated for a number of molecules [1–3], including metal (II) macrocyclic compounds (MPc) [4–12]. For metal (II) phthalocyanines adsorbed layers, the d-filling of the metal center atom is seen to alter the molecular band offsets [6–9], and in the case of the macrocyclic metal tetraazaannulenes (TMTAA), the d-filling of the metal center atom alters the preferential molecular orientation upon adsorption [12]. For the roughly spherical *closo*-carboranes, a clear relationship is observed between the dipole moment of the adsorbate and the alignment of the observed molecular orbitals with respect to the substrate Fermi level [3]. For smaller adsorbates, like N₂, similar effects are observed [13, 14], but the profound differences in substrate interaction tend to obscure the effect of the interface dipole itself. While the effects of the dipole moment along the surface normal are expected [1–3, 15, 16], the possible role of the in-plane dipole, the dipole of the adsorbate parallel with the interface, is far less clear [16].

One way to test for effect due to the in-plane adsorbate dipole is to compare the adsorption of planar molecules, with different dipole moments, on a substrate where the adsorbate interactions with the substrate are weak. With this goal, we have investigated the adsorption of the three different isomers of di-iodobenzene (C₆H₄I₂) on graphite surface at 110 K. Graphite has several advantages as a substrate for in-plane adsorbate dipole interactions. Graphite is a sub-

strate where the interactions with substituted benzene adsorbates are weak, and very flat surfaces can be prepared with very few steps. By avoiding surface steps we minimize the number of adsorbate interactions at step edges. The weak influence of the graphite substrate with the adsorbate is important in suppressing adsorbate dissociation, particularly as dehalogenation, seen with halogenated benzene adsorption, occurs on many substrates [17–20], but does not occur with initial halogenated benzene adsorption on some select metal [21–25] and nonmetallic substrates [26–28].

2. Experimental

Di-iodobenzene adsorption was performed with the graphite substrates cooled to 110 K, where C–I bond scission is unlikely [22–25], under ultra-high vacuum (UHV) conditions. The clean graphite surface was characterized by core level X-ray photoemission (XPS), and combined valence band photoemission and inverse photoemission, as described elsewhere [29]. An Al K_α ($h\nu = 1486.6$ eV) was used for the XPS studies with the electrons collected along the surface normal and analyzed in a hemispherical SCIENTA SES-100 electron energy analyzer. Throughout this work, the photon incidence angle was 45° off the surface normal. Binding energies are referenced throughout to the C 1s binding energy of the clean graphite surface at 284.3 ± 0.1 eV. Curve fitting was performed with CasaXPS using a standard XPS Gaussian–Lorentzian asymmetric line profile.

The isomers 1,2 (ortho), 1,3 (meta), and 1,4 (para) di-iodobenzenes along with 1-bromo 4-iodobenzene were purchased from Sigma–Aldrich. Each was introduced into the ultra-high vacuum chamber through a standard leak valve. Exposures are noted in

Langmuirs (1 L = 1 × 10⁻⁶ Torr sec) and reported as measured, uncorrected for ionization gauge cross-sections, unless noted specifically otherwise.

3. Apparent sticking coefficients

With di-iodobenzene adsorption on graphite at 110 K, the benzene backbone contributes a new C 1s core level feature initially at binding energies of 285.2 + 0.2 and 284.8 + 0.2 eV for 1,2 (ortho), and 1,4 (para) di-iodobenzene, respectively, as shown in Figure 1. In addition to the C 1s core level associated with graphite, there is an adsorbate induced C 1s core level feature at 285.5 + 0.2 eV binding energy with the initial exposure for 1,3 (meta), di-iodobenzene adsorbed on graphite at 110 K. For all of the different isomers, these core level binding energies increase with increasing

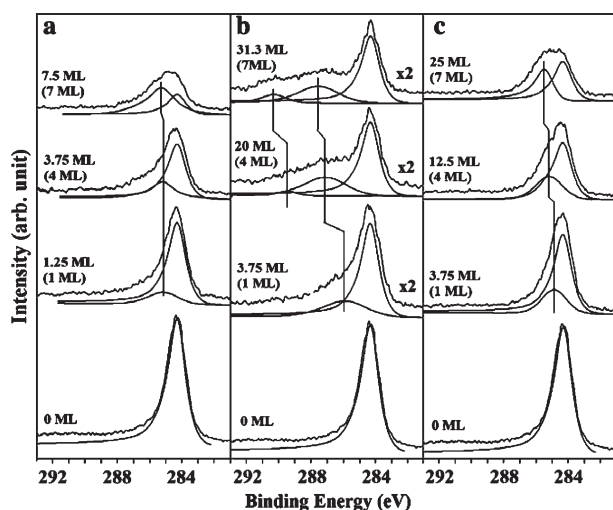


Figure 1. The X-ray photoemission spectra in the region of the C 1s from (a) 1,2-di-iodobenzene, (b) 1,3-di-iodobenzene, (c) 1,4-di-iodobenzene adsorbed on graphite at 110 K, for different exposures. Black curves represent the photoemission spectra and thin lines indicate the various components of spectra, modeled using a standard XPS Gaussian-Lorentzian asymmetric line profile. The feature (component) at 284.3 eV binding energy can be assigned to the substrate graphite. Coverages are indicated assuming the same initial sticking coefficient for each isomer (see text) as well as the apparent coverage based on the fittings to the attenuation of the substrate signal (see text), denoted in the brackets.

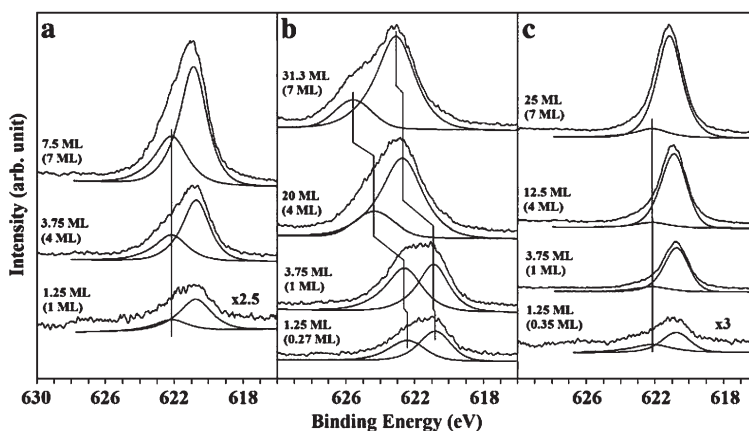


Figure 2. The X-ray photoemission spectra in the region of the iodine 3d_{5/2} from (a) 1,2-di-iodobenzene, (b) 1,3-di-iodobenzene, (c) 1,4-di-iodobenzene adsorbed on graphite at 110 K, for different exposures. Black curves represent the photoemission spectra and thin lines indicate the various components of spectra, modeled using a standard XPS Gaussian-Lorentzian asymmetric line profile. Coverages are indicated assuming the same initial sticking coefficient for each isomer (see text) as well as the apparent coverage based on the fittings to the attenuation of the substrate signal (see text), denoted in the brackets.

exposure and 1,2 (ortho), 1,3 (meta), and 1,4 (para) di-iodobenzene coverage (Figure 1).

As indicated in Figure 2, the expected iodine 3d_{5/2} core level is evident initially at a binding energy of 620.7 + 0.1 eV for all three isomers, and like the di-iodobenzene induced C 1s core level contributions to the XPS spectra, also increases in binding energy with increasing coverage, as discussed below. For submonolayer coverages of 1,3 (meta), and multilayer coverages of 1,2 (ortho) di-iodobenzene, a second I 3d_{5/2} core level is observed at binding energies significantly greater than 622 eV, as discussed below. A second I 3d_{5/2} core level peak is also observed for 1,4 (para) di-iodobenzene, but is a weak feature and more difficult to identify without the aid of core level photoemission line shape analysis.

From the attenuation of the distinct substrate graphite C 1s core level at a binding energy of 284.3 + 0.1 eV, and the increase of the iodine 3d_{5/2} core level signal intensities, we can make an estimate of the apparent di-iodobenzene coverages. Fitting that assume a uniform growth model, have been assumed, as noted elsewhere, as indicated in Figure 3. For these estimates we assume that the electron mean free path for photoelectrons emitted from the C 1s core edge to be about 11 Å [30], and may be longer given that the molecular overlayer is insulating providing no plasmon decay mechanisms for inelastic scattering. These simplified assumptions yield an apparent sticking coefficient of 0.178 for 1,2-di-iodobenzene, 0.0385 for 1,3-di-iodobenzene, and 0.049 for 1,4-di-iodobenzene.

These sticking coefficients S assume the linear relation between the exposure x and coverage y :

$$y = (S/q) \times (x/x_0)$$

where x_0 is the exposure needed to form one monolayer of coverage (roughly 8 × 10¹⁸ molecules/m²) and q is the ratio of adsorbate ionization cross-section to that of N₂. We have assumed that in fact the ionization gauge cross-section of di-iodobenzene is likely to be much higher than for nitrogen; for example toluene ionization gauge cross-section is 6.4 times greater than nitrogen [31] while benzene has an ionization gauge cross-section that is a factor of 3.5 [31] to 5.7 [32] greater than nitrogen. Based on the ionization cross-sections of these similar molecules, we have assumed that the ionization gauge sensitivities for di-iodobenzenes are in the region of $q = 6$, though higher values might well be possible.

The actual sticking coefficients, as opposed to the apparent molecular sticking coefficients computed based on a uniform layer-by-layer growth model, may be approximately the same for all three

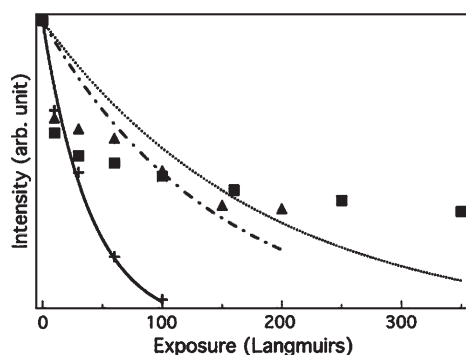


Figure 3. The intensity of graphite substrate core level C 1s feature, at 284.3 eV binding energy, as a function of exposure to (+) 1,2-di-iodobenzene, (■) 1,3-di-iodobenzene, (▲) 1,4-di-iodobenzene, in Langmuirs (1 L = 1×10^{-6} Torr sec), with pressures and plotted exposures uncorrected for ionization gauge cross-section(s).

isomers of di-iodobenzene. There is a strong similarity in the initial decay of the graphite substrate intensities for all three isomers with initial di-iodobenzene exposure from 0 L to 10 L, as indicated in Figure 3. Thus the overall sticking coefficients of all of the di-iodobenzene isomers may, in fact, be similar to that of 1,2-di-iodobenzene, which exhibits the highest sticking coefficient overall and the behavior that most closely resembles layer-by-layer growth. The correspondences between the nominal coverage and the measured exposure are 1 monolayer (ML) corresponding to 8 L for 1,2-di-iodobenzene, 1 ML corresponding to 37 L for 1,3-di-iodobenzene, and 1 monolayer corresponding to 29 L for 1,4-di-iodobenzene, with the apparent sticking coefficients abstracted from the decrease in substrate signal and stated pressures and exposure, as measured and uncorrected for ionization gauge cross-section.

In fact, only 1,2 (ortho) di-iodobenzene exhibits the exponential decay of the graphite substrate signal that is characteristic of uniform growth of the molecular overlayer (Figure 3). For the isomers 1,3- and 1,4-di-iodobenzene, the decay of graphite intensities does not follow the expected exponential decline in intensities after 10 L (as measured and uncorrected for ionization gauge cross-section). This behavior indicates that the isomers 1,3- and 1,4-di-iodobenzene molecular films adopt a Stranski-Krastanov or Volmer-Weber (island) growth mode, as discussed in greater detail below. A Stranski-Krastanov or Volmer-Weber growth mode results in an apparent sticking coefficient and a concomitant

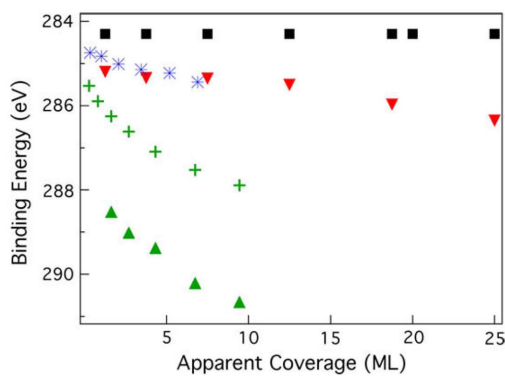


Figure 4. The X-ray photoemission C 1s core level binding energies for (▼) 1,2-di-iodobenzene, (+, ▲) 1,3-di-iodobenzene, (⊕) 1,4-di-iodobenzene as a function of coverage. Coverages are nominal or apparent coverages based on the attenuation of the graphite substrate C 1s core level feature at 284.3 eV binding energy (see text). The common graphite substrate core level C 1s binding energy, at 284.3 eV (■), is shown for reference.

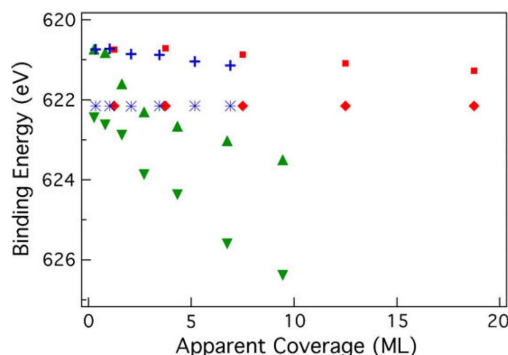


Figure 5. The X-ray photoemission I $3d_{5/2}$ core level binding energies for (■, ♦) 1,2-di-iodobenzene, (+, ⊕) 1,4-di-iodobenzene, (▲, ▼) 1,3-di-iodobenzene as a function of coverage. Coverages are nominal coverages based on the attenuation of the graphite substrate C 1s core level feature at 284.3 eV binding energy (see text).

apparent coverage that may, in fact, be much smaller than the real or true sticking coefficient as measured by our techniques.

The strong tendency to adopt a Volmer-Weber (island) growth mode for meta 1,3-di-iodobenzene adsorption on graphite at 110 K is evident in the C 1s core level binding energies and the iodine $3d_{5/2}$ core level binding energies plotted as a function of apparent coverage, in Figures 4 and 5, respectively. While the core level binding energies for 1,2 (ortho), and 1,4 (para) di-iodobenzene are very similar when rescaled according to apparent coverage (not exposure), 1,3 (meta) di-iodobenzene remains distinctly different, with far greater core level binding energies. The possibilities for the differences in the observed core level binding energies between the various isomers are limited. In a sense, it is clear that para 1,4-di-iodobenzene has far more uniform initial growth of the molecular film (as indicated in Figure 4, although not as uniform as 1,3-di-iodobenzene, as indicated in Figure 3), and thus follows a Stranski-Krastanov growth mode, and tends not to grow in a more extreme island growth mode that would more resemble the Volmer-Weber growth mode as appears to be the tendency for meta 1,3-di-iodobenzene (Figures 4 & 5).

The least likely scenario is that there is distinctly different adsorption chemistry that occurs for 1,3 (meta) di-iodobenzene compared to 1,2 (ortho), and 1,4 (para) di-iodobenzene adsorption on graphite; our model density functional theory calculations provide no indication that this would or should be the case. Intermolecular interactions and different growth modes that vary with isomer are therefore the most likely origin of the differences observed for 1,3 (meta) di-iodobenzene compared to 1,2 (ortho), and 1,4 (para) di-iodobenzene adsorption on graphite at 110 K.

4. Screening

For 1,3-di-iodobenzene, the coverage dependent XPS spectra show very large shifts in both the C 1s and I 3d core level features, as we have indicated. These increases in core level binding energies of ~3 eV or more are far greater than core level shifts observed for 1,2- and 1,4-di-iodobenzene (Figure 4 and Figure 5). Since dissociative chemisorption can be excluded in all of the adsorption systems we describe here, such large core level shifts can only result from strong intermolecular interactions or decreased screening from the graphite substrate, resulting in larger photoemission final state binding energies [33–37].

The increases in the C 1s core level binding energy with increasing adsorbate coverages are certainly consistent with decreasing final state screening of the adsorbate molecular layers with increased multilayer growth [35–37]. In addition, di-iodobenzene residing in a molecular multilayer could well provide a sec-

ond iodine 3d_{5/2} core level photoemission feature at a significantly higher binding energy as is observed for ortho 1,2- and meta 1,3-di-iodobenzene (Figure 2). This additional I 3d core level feature is only apparent at coverages greater than nominally one monolayer or approaching one nominal monolayer for ortho 1,2-di-iodobenzene and meta 1,3-di-iodobenzene. The two I 3d core level features for ortho 1,2- and meta 1,3-di-iodobenzene adsorption appear too close in binding energy to be attributable to the spin-orbit I 3d_{3/2} and I 3d_{5/2} companions individually [38–41].

Accordingly, we can partially (but not completely) attribute these different I 3d_{5/2} core level features to the differences in screening between the monolayer (with the I 3d_{5/2} core level binding energies appearing at 620.7 ± 0.1 eV to 621.3 ± 0.4 eV in the case of ortho 1,2-di-iodobenzene) and multilayer growth of 1,2-di-iodobenzene (622.2 ± 0.3 eV binding energy). This explanation is, however, incomplete. The iodine 3d_{5/2} core level photoemission feature that is initially observed at a binding energy of 620.7 ± 0.1 eV for all three isomers, increases in both intensity and binding energy for all three isomers with increasing di-iodobenzene coverage, as indicated in Figure 2 and Figure 5. This change in the initial I 3d_{5/2} core level binding energy, with increasing di-iodobenzene coverage, is not the expected behavior of a core level feature whose origin arises solely from molecules restricted to the interface of a molecular film of increasing thickness.

The most dramatic changes observed for the I 3d_{5/2} core level binding energies are seen with 1,3-di-iodobenzene on graphite at 110 K. These binding energy shifts include the component of the I 3d_{5/2} core level that is initially observed at a binding energy of 620.7 ± 0.1 eV. There is thus a need to invoke intermolecular interactions that can include intermolecular screening [11, 42], chemical shifts due to intermolecular hybridization [43], as well as final state effects attributable to screening from the substrate [33, 34].

If the I 3d feature observed at a binding energy of 620.7 ± 0.1 eV for all three isomers is solely attributable to the first molecular monolayer, then we should see the *decrease* in intensity for emission from this lower binding energy feature simply because the photoemission intensities for the first layer should decrease as it is buried beneath the additional adsorbed multilayers. The significant shifts in core level binding energy observed for all the components of the I 3d core level observed in XPS, for the meta 1,3-di-iodobenzene (Figures 4 & 5), while very little coverage dependent changes are seen for para 1,4-di-iodobenzene, tend to implicate the existence of very strong intermolecular interactions and/or the chemical shifts.

The shift in the I 3d_{5/2} core level binding energy partially attributed to the first monolayer is likely partly due to interface dipole changes [44], and changes in the dipole layer interaction as the film thickness increases. We cannot assign one of the di-iodobenzene I 3d_{5/2} core level features to simply a well screened interface molecular species because of the coverage dependent binding energies and intensity increases. These issues and the presence of two distinct peaks in the I 3d_{5/2} core level photoemission spectra require consideration of intermolecular interactions and/or the chemical shifts with the growth of the molecular film.

As just noted, the shift towards increasing binding energies for the two I 3d_{5/2} features observed for meta 1,3-di-iodobenzene are very significant (Figure 5), with the feature at greater binding energies exhibiting even greater increases in binding energy with increasing 1,3-di-iodobenzene coverages. These strong differences for the two I 3d_{5/2} features observed for meta 1,3-di-iodobenzene adsorption suggest strong intermolecular interactions, in addition to the effect of the substrate on final state photoemission screening and molecular polarization [33–36]. Some of the similar observations based on the C 1s core level spectra (Figure 4) also are consistent with the need to invoke intermolecular interactions particularly for meta 1,3-di-iodobenzene.

As noted in the prior section, meta 1,3-di-iodobenzene isomer adopts a growth mode on graphite at 110 K very close to Volmer-Weber growth. Such a growth mode is consistent with the huge core level binding energy shifts, and the persistence of the graphite C 1s core level 284.3 ± 0.1 eV binding energy feature even when the iodine 3d_{5/2} features for meta 1,3-di-iodobenzene are of very significant intensities. At similar at iodine 3d_{5/2} intensities for 1,2- and 1,4-di-iodobenzene the graphite C 1s core level intensities are quite weak. Intermolecular interactions are necessary to explain the strongly coverage dependent multiple iodine 3d_{5/2} and C 1s core level features at widely different binding energies and the tendency for strongly island like molecular thin film growth of the meta 1,3-di-iodobenzene adlayer. Such intermolecular interactions may actually have an origin in the frontier orbitals of di-iodobenzene, and thus may be partly related to geometrical considerations.

5. Geometry effects in di-iodobenzene packing

It is important to exclude simple statistical differences in the molecular packing of the different di-iodobenzenes. Geometry of molecular packing can play an important role in substituted arene adsorbate interactions [44–46]. Isomeric effects have been observed with halogenated benzenes due to substrate interactions [45] and intra-molecular substituent proximity effects [25], but strong intermolecular interactions are to be expected as well [46].

Because of the difference in the relative positions of two iodine molecules in each isomer, each isomer must have certain preferential directions favored for adoption in the adsorption process. From purely geometrical point of view, we have calculated the number of possible ways the crystal can be arranged in the periodic manner without forming I-I bond between adjacent molecules for 1, 2, and 3 molecules per basis (molecular building block aggregate), considering a close packed geometry of di-iodobenzenes (Table 1) as well as 1, 2, and 3, and 4 molecules per basis (molecular building block aggregate) with pair-wise hydrogen bonding (Table 2). Other planar packing geometries for di-iodobenzenes and like molecules are possible, but these two types of packing geometries are illustrative of the overall role of geometry. Both of these packing geometries for the di-iodobenzenes are schematically illustrated in Figure 6.

Table 1. The result of geometrical analysis of crystal formation, assuming a close packed geometry, for each isomer of di-iodobenzene. The number of possible arrangements is listed for each unit cell specified the number of molecules and possible “holes” (see text). See Figure 6a and b for the depiction of packing geometries with no “hole” and with a hole in the unit cell lattice respectively.

Number of molecules per basis	1		2		3			
	CP	CP	1 hole	Total	CP	1 hole	2 holes	Total
Number of lattice-basis combinations	1	1	1	2	3	2	1	6
1,2	1	20	15	35	56	72	64	192
1,3	0	8	18	26	5	72	72	149
1,4	1	17	12	29	156	80	80	316

Table 2. The result of geometrical analysis of crystal formation assuming pair-wise hydrogen interactions, for each isomer of di-iodobenzene. The number of possible arrangements is listed for each unit cell specified the number of molecules and possible "holes" (see text). See Figure 6c and d for an indication of the overall packing geometries with no "hole" and with a hole in the unit cell lattice respectively.

Number of molecules per basis	1		2		3			Total
	CP	CP	1 hole	Total	CP	1 hole	2 holes	
Number of lattice-basis combinations	1	1	1	2	3	2	1	6
1,2	1	22	24	46	246	188	120	554
1,3	1	22	27	49	246	196	142	584
1,4	0	8	24	32	48	256	128	432

Number of molecules per basis	4						Total
	CP	1 hole	2 holes	3 holes	4 holes	Total	
Number of lattice-basis combinations	5	4	4	2	2	17	
1,2	1556	1592	1980	1248	1216	7592	
1,3	1612	1848	2218	1488	1488	8654	
1,4	1056	1568	2304	1408	1408	7744	

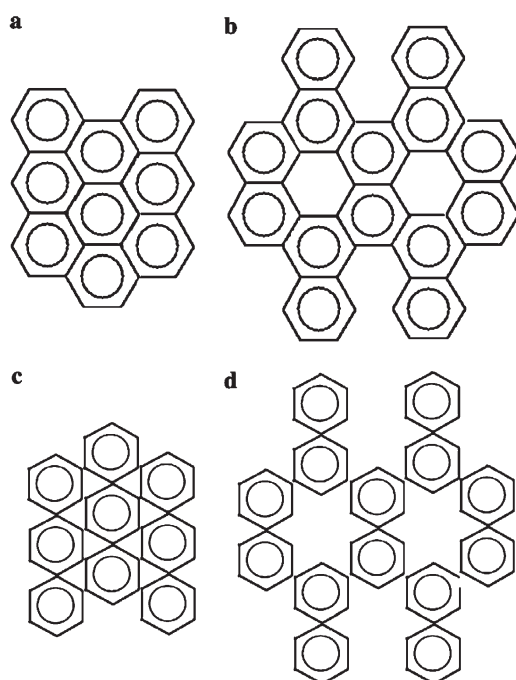


Figure 6. The depiction of (a) close packed and (b) corresponding one-hole structures indicating some of the packing arrangements considered in Table 1 as well as a depiction of (c) the pair-wise dense but not close packed and (d) corresponding one-"hole" structures that are among some of the possible unit cell packing structures considered in Table 2.

Since the number of possible arrangements for certain molecule could be closely related to the probability of sticking, we have calculated the overall number of possible packing arrangements assuming that the molecules are arranged in the ideal Bravais lattice, but without considering the possible rotational symmetries with respect to the substrate. Although imposing this assumption may not be perfectly valid for the real crystal, by considering up to 4 molecules per basis we increase the periodicity of Bravais lattice, though each molecule in planar (two-dimensional) group may and will not preserve the Bravais lattice relaxing the overall constraints.

Let us begin our consideration of the statistical role of the planar packing geometrical effects with the more close packed arrange-

ment of molecules (Figure 6a & b). The result of these simple summations of possible packing arrangements is shown in the Table 1. If the in-plane packing is completely close packed, the meta 1,3-di-iodobenzene cannot form a Bravais lattice, and this alone may favor growth or a more "vertical" molecular structure than an "in-plane" close packed structure. As indicated in Table 1, this tendency appears to hold well for unit cells with planar arrangements that contain 2 and more molecules, unless there is a "hole" in the packing arrangement, as indicated in Figure 6b. A hole in the unit cell lattice would be tantamount to "inverse" Volmer-Weber growth.

For greater completeness, we have also considered an in-plane packing of di-iodobenzenes based on pair-wise hydrogen interactions (Figure 6c & d). From Table 2, it can be easily surmised that 1,4-di-iodobenzene is generally least likely to form a pair-wise packing structure with any number of molecules per basis and prefers to form the periodic structure with the unfilled holes left on the layer. For the meta 1,3-di-iodobenzene, the total number of possible packing arrangements is the highest among all the isomers (in our analysis for up to 4 molecules per basis), when considering a pair-wise packing structure, but in general (not always) this is a result of the fact that the available packing arrangements for meta 1,3-di-iodobenzene is very high when one allows for "holes" in the unit cell lattice. For example, since the probability of forming the structure with holes (not immediately close packed in a two-dimension grouping) is high for the meta 1,3-di-iodobenzene, this could enhance the tendency for this isomer to form "inverse" islands, that is to say "holes" in the molecular film.

These geometrical packing models suggests that the probability of the sticking is highest for 1,3-di-iodobenzene when there is either "inverse" Volmer-Weber growth, i.e. "holes" in the molecular unit cell, or there is island growth (more conventional growth that resembles Volmer-Weber growth). Although both meta 1,3- and para 1,4-di-iodobenzene exhibit the departure from a pure exponential decay of the substrate graphite intensities, with increasing film growth, just the available number of packing possibilities for the various isomers may play some role in the difference in their sticking coefficients.

From the graphite core level intensities, the apparent sticking coefficients of three isomers (uncorrected for the growth mode) rank from largest to smallest, ortho 1,2-di-iodobenzene, para 1,4-di-iodobenzene, to meta 1,3-di-iodobenzene supporting the conclusion that 1,3-di-iodobenzene grows in a mode that more closely resembles Volmer-Weber growth. Because of the growth mode that tends strongly towards Volmer-Weber island growth or "inverse" Volmer-Weber growth, containing a high density of "holes", meta 1,3-di-iodobenzene appears to exhibit much smaller

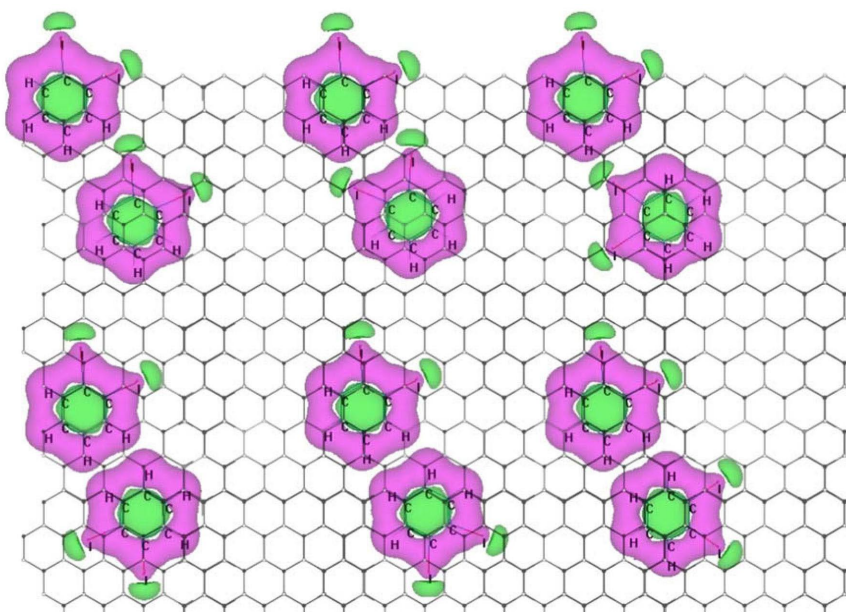


Figure 7. A schematic representation of different pair-wise arrangements of ortho 1,2-di-iodobenzene on graphite. For the purposes of this schematic, one molecule is placed in registry with the graphite substrate, and for the six possible pair-wise arrangements, only half allow the second di-iodobenzene to remain in registry with the substrate. A largely σ -bonding electron cloud has been chosen for this schematic (see text).

sticking coefficient, smallest in three isomers, based in part on the exponential curve fitting from the decreasing substrate intensity. This low apparent sticking coefficient may not be representative of the true sticking coefficient whose value, as suggested by our geometrical models, may in fact be larger than for the other isomers. In fact, strong intermolecular interactions must still be invoked to explain the significant differences in the growth mode and coverage dependent core level binding energies observed for meta 1,3-di-iodobenzene compared to that seen for 1,2- and 1,4-di-iodobenzene. Geometrical effects alone cannot be used to explain all of core level binding energy results. The phenyl coupling reaction indicates that substituted meta (1,3) iodobenzenes do have strong intermolecular interactions [46].

These geometrical considerations (just discussed above) do not consider the graphite substrate and possible registry of the di-iodobenzene with the substrate. Such substrate interactions that would favor registry with the graphite substrate would likely occur through the arene π molecular orbitals. The spacings between di-iodobenzene molecules are dominated by the frontier σ molecular orbitals. The actual adsorbate size and spacing between di-iodobenzene will depend upon the intermolecular interactions and relative orientations, but as seen in Figure 7 for 1,2-di-iodobenzene, only a few pair interaction would be likely to allow adjacent di-iodobenzene molecules to remain in registry with the graphite substrate. In fact, with a two-dimensional space filling packing arrangement, not all di-iodobenzene molecules can be placed in registry with the graphite substrate. Such registry possible with the graphite substrate comes from superlattice periodicity, and this in turn depends on the packing arrangement adopted by the di-iodobenzene. Without a two-dimensional space filling packing arrangement, more di-iodobenzene adsorbate registry with the graphite substrate is certainly possible. Structural studies, such as scanning tunneling microscopy, are indicated to resolve these local intermolecular structural issues.

6. Isomer effects versus dipole interaction

In fact, each isomer of di-iodobenzene exhibits a different electric dipole in the plane of the benzene ring. We have strived to

distinguish between intermolecular interaction caused by the different arrangements of substitutions, possible as indicated by the geometrical considerations just discussed previously, and possible dipole effects that are not simply a result of different substitution geometries. In an effort to explore a distinction between these two effects, we have compared para 1,4-di-iodobenzene with 1-bromo,4-iodobenzene. These two molecules have similar geometric substitutions, but the latter has a small net electric dipole in the plane of the benzene ring due to differences in the halogen substitutions while the former has no net electric dipole moment. It must be understood at the outset that an assignment of intermolecular interactions to one single effect alone is not possible and any attempt to do so is very open to many criticisms. Of course the substitution geometries and electric dipole magnitudes are interlinked, as are many other phenomena.

Despite the identical positions of halogen substitution, these two molecules exhibit very distinct apparent sticking coefficients. The apparent sticking coefficient for 1,4-di-iodobenzene (as noted previously) was found to be 0.049 while the value is 0.13 for 1-bromo, 4-iodobenzene, as estimated by the diminution of graphite substrate intensities (Figure 8) and based again on assuming that

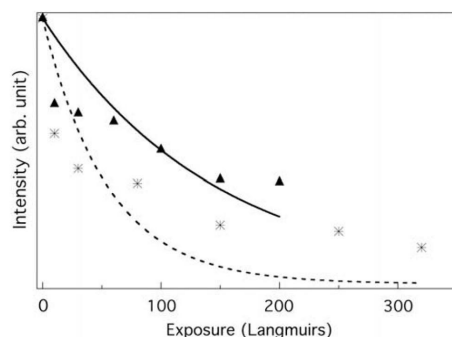


Figure 8. The intensity of graphite substrate core level C 1s feature, at 284.3 eV binding energy, as a function of exposure to (\blacktriangle) 1,4-di-iodobenzene and ($*$) 1-bromo, 4-iodobenzene in Langmuirs (1 L = 1×10^{-6} Torr sec), with pressures and plotted exposures uncorrected for ionization gauge cross-section(s).

the ionization gauge sensitivities to di-iodobenzenes are in the region of $q = 6$, though higher values again might well be possible. As seen in Figure 8, the decay in substrate intensities more closely fits an exponential profile for 1-bromo, 4-iodobenzene than is the case for 1,4-di-iodobenzene adsorption on graphite at 110 K. This is particularly true for exposures greater than 10 L (uncorrected for ionization gauge cross-section). Indeed, the apparent sticking coefficient of 0.13 for 1-bromo, 4-iodobenzene approaches the value of 0.178 noted for 1,2-di-iodobenzene. For the nominal apparent 1 ML coverage, there is a contrast between the associated measured exposure of 29 L for 1,4-di-iodobenzene and the corresponding 11 L exposure associated with 1-bromo, 4-iodobenzene, based on the calculated apparent sticking coefficients but uncorrected for growth mode. These results tend to indicate that 1-bromo, 4-iodobenzene adsorption on graphite more closely resembles the layer-by-layer growth mechanisms of 1,2-di-iodobenzene than the Volmer-Weber (island) growth mode adopted by 1,3-di-iodobenzene on graphite.

The C 1s spectra of 1-bromo, 4-iodobenzene characterized initially by two peaks at 284.7 ± 0.2 eV and 286.1 ± 0.2 eV are apparent with the initial exposure of 10 L, as seen in Figure 9. The lower binding energy feature of 1-bromo, 4-iodobenzene is close to the di-iodobenzene adsorbate C 1s feature at a binding energy of 284.8 ± 0.2 eV observed with the initial adsorption of both 1,4-di-iodobenzene and 1,2-di-iodobenzene on graphite, as noted previously. The higher binding energy feature is not entirely unexpected given that bromine has a much higher electron affinity than iodine.

The increase in binding energy of the 1-bromo, 4-iodobenzene C 1s core level feature at 284.7 ± 0.2 eV with increasing coverage resembles that observed for 1,2-di-iodobenzene, as summarized in Figures 10 & 4, respectively. These results combined all indicate that the growth mode of 1-bromo, 4-iodobenzene approaches a layer-by-layer growth mode far better than we observe for 1,4-di-iodobenzene adsorption on graphite. The implication is that intermolecular interactions of 1-bromo, 4-iodobenzene are likely more similar to that of 1,2-di-iodobenzene than 1,4-di-iodobenzene.

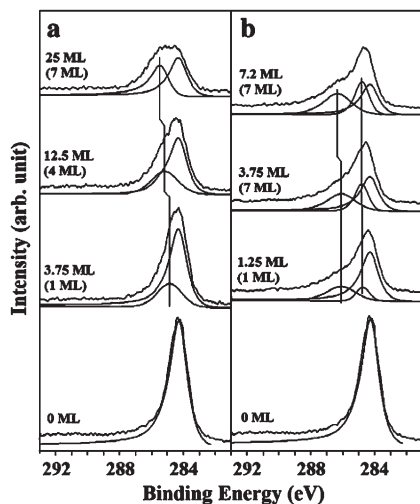


Figure 9. The X-ray photoemission spectra in the region of the C 1s from (a) 1,4-di-iodobenzene, (b) 1-bromo, 4-iodobenzene adsorbed on graphite at 110 K, for increasing exposures and coverages. Black curves represent the photoemission spectra and thin lines indicate the various components of spectra, modeled using a standard XPS Gaussian-Lorentzian asymmetric line profile. The common feature (component) at 284.3 eV binding energy can be assigned to the graphite substrate. Coverages are indicated assuming the same initial sticking coefficient for each isomer (see text) as well as the apparent coverage based on the fittings to the attenuation of the substrate signal (see text), denoted in the latter case in brackets.

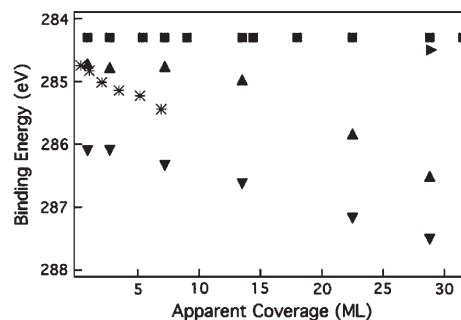


Figure 10. The X-ray photoemission C 1s core level binding energies for (▲) 1,4-di-iodobenzene and (▼) 1,4-bromiodobenzene as a function of coverage. Coverages are nominal or apparent coverages based on the attenuation of the graphite substrate C 1s core level feature at 284.3 eV binding energy (see text). The common graphite substrate core level binding energy C 1s binding energy, at 284.3 eV, (■) is shown for reference.

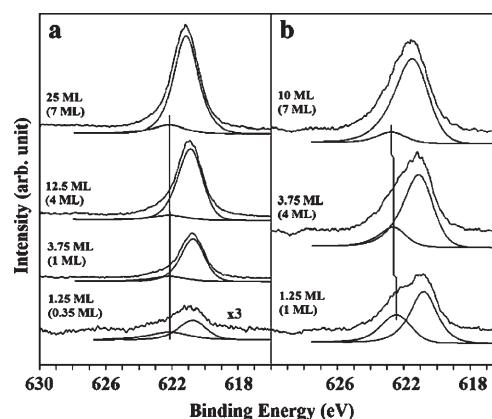


Figure 11. The X-ray photoemission spectra in the region of the iodine $3d_{5/2}$ from (a) 1,4-di-iodobenzene, (b) 1-bromo, 4-iodobenzene adsorbed on graphite at 110 K, for increasing exposures and coverages. Black curves represent the photoemission spectra and thin lines indicate the various components of spectra, modeled using a standard XPS Gaussian-Lorentzian asymmetric line profile. Coverages are indicated assuming the same initial sticking coefficient for each isomer (see text) as well as the apparent coverage based on the fittings to the attenuation of the substrate signal (see text), denoted in the latter case in brackets.

As indicated in Figure 11, the iodine $3d_{5/2}$ core level photoemission peaks for initial 1-bromo, 4-iodobenzene adsorption on graphite at 110 K were observed at 620.8 ± 0.2 eV and 622.5 ± 0.2 eV at 10 L exposure (uncorrected for ionization gauge cross-section). The smaller binding energy I 3d feature for 1-bromo, 4-iodobenzene adsorbed on graphite (Figure 11) does resemble the initial I $3d_{5/2}$ binding energy feature observed at 620.7 ± 0.1 eV at 1,2-di-iodobenzene (Figure 2). There are greater increases in the iodine $3d_{5/2}$ core level photoemission binding energies with increasing coverages and exposure to 1-bromo, 4-iodobenzene, than were observed for 1,4-di-iodobenzene, as seen in Figure 11 and summarized in Figure 12. These more dramatic increases in the iodine $3d_{5/2}$ core level photoemission binding energies for increasing coverages of 1-bromo, 4-iodobenzene (Figure 12) on graphite resemble that observed for 1,3-di-iodobenzene (Figure 5). While this might appear to be difficult to reconcile with a growth mode that approaches layer-by-layer growth for 1-bromo, 4-iodobenzene adsorption on graphite, we recognize that the frontier orbitals for iodine extend farther from the benzene molecular backbone than is the case of bromine. The large shifts in

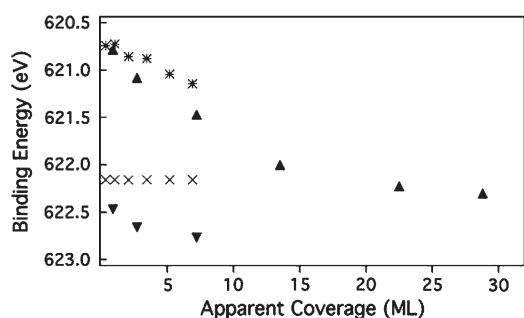


Figure 12. The X-ray photoemission I $3d_{5/2}$ core level binding energies for (*, ×) 1,4-di-iodobenzene, (▲, ▼) 1,4-bromiodobenzene as a function of coverage. Coverages are nominal or apparent coverages based on the attenuation of the graphite substrate C 1s core level feature at 284.3 eV binding energy (see text).

the I 3d core level spectra indicate that the dipolar interactions between molecules do lead to some of the apparent chemical shifts. The spatial extent of frontier molecular orbitals (i.e. the “electron cloud”, as schematically indicated in Figure 7) of bromine differ from those molecular orbital with strong iodine weight and likely contribute to some of the effects observed.

The overall results imply the in-plane molecular dipoles do affect the growth mode of the molecular film and intermolecular interactions. The loss of symmetry from C_{2v} to C_{1h} , an adsorbed molecule with only one mirror plane, is a complication that can not be excluded from this comparison of 1,4-di-iodobenzene with 1-bromo, 4-iodobenzene adsorption on graphite. Although 1,4-di-iodobenzene has a point group symmetry of D_{2h} , as a free molecule, the dihedral mirror plane symmetry is lost with adsorption, i.e. there is a symmetry reduction for an adsorbed molecule to two mirror planes and the C_2 rotation operation, even without consideration of the site and symmetry of the substrate. As has been seen here in the comparison of 1-bromo, 4-iodobenzene with 1,4-di-iodobenzene, the suggestion that benzene substitutions have an effect on the intermolecular interactions may also be evident in the comparison of fluoroiodobenzene isomers with iodobenzene and iodotoluene adsorption on Cu(1 1 1) [46]. In the case of the latter study symmetry effects must play a much diminished role in adsorption as the overall molecules symmetries are low for all of the adsorbates studied.

7. Summary

In the case of di-iodobenzene adsorption on graphite, as reported here, and the adsorption of fluoroiodobenzene adsorption on Cu(1 1 1) [46] and chlorobenzenes on Si(1 0 0) [45], reported previously, it is very clear that the choice of isomer does affect the adsorption and desorption of the adsorbate. In the case of di-iodobenzene adsorption on graphite, there are clear indications that the isomer not only affects the intermolecular interactions significantly, but also affects the growth mode. Some of this influence of the choice of isomer must be attributed to the in-plane electric dipole, as indicated by the comparison with 1-bromo, 4-iodobenzene, but it cannot be dipole interactions alone that influence the intermolecular interactions as meta 1,3-di-iodobenzene deviates from a layer-by-layer molecular growth mode more than we observe for both para 1,4-di-iodobenzene and ortho 1,2-di-iodobenzene.

Clearly what is indicated is the need for future studies in which atomic resolution atomic force microscopy is combined with photoemission, so that detailed information on growth and electronic structure may be simultaneously compared, as in studies of the large aromatic planar molecular species [47, 48].

Acknowledgments

This research was supported by the National Science Foundation through Grant No. CHE-0650453. The authors thank R.G. Jones and Bruce A. Parkinson for a number of helpful discussions.

References

- [1] H. Ishii, K. Sugiyama, E. Ito and K. Seki, *Adv. Mater.* **11** (1999), p. 605.
- [2] X.Y. Zhu, *Surf. Sci. Rep.* **56** (2004), p. 1.
- [3] S. Balaz, A.N. Caruso, N.P. Platt, D.I. Dimov, N.M. Boag, J.I. Brand, Ya.B. Losovjy and P.A. Dowben, *J. Phys. Chem. B* **111** (2007), p. 7009.
- [4] S. Kera, Y. Yabuuchi, H. Yamane, H. Setoyama, K.K. Okudaira and N. Ueno, *Phys. Rev. B* **70** (2004), p. 085304.
- [5] J. Xiao, A. Sokolov and P.A. Dowben, *Appl. Phys. Lett.* **90** (2007), p. 242907.
- [6] X. Lu, K.W. Hipps, X.D. Wang and Ursula Mazur, *J. Am. Chem. Soc.* **118** (1996), p. 7197.
- [7] X. Lu and K.W. Hipps, *J. Phys. Chem. B* **101** (1997), p. 5391.
- [8] J. Xiao and P.A. Dowben, *J. Phys. Condens. Matter* **21** (2009), p. 052001.
- [9] J. Xiao and P.A. Dowben, *J. Mater. Chem.* **19** (2009), p. 2172.
- [10] P.A. Dowben, Jie Xiao, Bo Xu, Andrei Sokolov and B. Douidin, *Appl. Surf. Sci.* **254** (2008), p. 4238.
- [11] P.A. Dowben, L.G. Rosa, C.C. Ilie, Jie Xiao, *J. Electron Spectrosc. Relat. Phenom.* (2009), doi: 10.1016/j.elspec.2009.03.005.
- [12] J. Liu, J. Xiao, S.-B. Choi, P. Jeppson, L. Jarabek, Ya.B. Losovjy, A.N. Caruso and P.A. Dowben, *J. Phys. Chem. B* **110** (2006), p. 26180.
- [13] N.D. Shinn, *Phys. Rev. B* **41** (1990), p. 9771.
- [14] N.D. Shinn and K.-L. Tsang, *J. Vac. Sci. Technol. A* **8** (1988), p. 2449.
- [15] V.S. L'vov, R. Naaman, V. Tiberkevich and Z. Vager, *Chem. Phys. Lett.* **381** (2003), p. 650.
- [16] D. Cahen, R. Naaman and Z. Vager, *Adv. Funct. Mater.* **15** (2005), p. 1571.
- [17] A.F. Lee, Z.P. Chang, S.F.J. Hackett, A.D. Newman and K. Wilson, *J. Phys. Chem. C* **111** (2007), p. 10455.
- [18] A.F. Carley, M. Coughlin, P.R. Davies, D.J. Morgan and M.W. Roberts, *Surf. Sci.* **555** (2004), p. L138.
- [19] M.X. Yang, M. Xi, H. Yuan, B.E. Bent, P. Stevens and J.M. White, *Surf. Sci.* **341** (1995), p. 9.
- [20] D.M. Jaramillo, D.E. Hunka and D.P. Land, *Surf. Sci.* **445** (2000), p. 23.
- [21] X.-L. Zhou and J.M. White, *J. Chem. Phys.* **92** (1990), p. 5612.
- [22] H. Cabibil, H. Ihm and J.M. White, *Surf. Sci.* **447** (2000), p. 91.
- [23] D. Syomin and B.E. Koel, *Surf. Sci.* **490** (2001), p. 265.
- [24] M. Xi and B.E. Bent, *Surf. Sci.* **278** (1992), p. 19.
- [25] B.M. Haines and J.L. Gland, *Surf. Sci.* **602** (2008), p. 1871.
- [26] S.C. Petitto, E.M. Marsh and M.A. Langell, *J. Phys. Chem. C* **110** (2006), p. 1309.
- [27] X.H. Chen, Q. Kong, J.C. Polanyi, D. Rogers and S. So, *Surf. Sci.* **340** (1995), p. 224.
- [28] L. Bugyi, A. Oszko and F. Solymosi, *Surf. Sci.* **539** (2003), p. 1.
- [29] J. Xiao, C. Ilie, N. Wu, K. Fukutani and P.A. Dowben, *Surf. Sci.* **603** (2009), p. 513.
- [30] A. Jablonski and C.J. Powell, *Surf. Sci. Rep.* **47** (2002), p. 33.
- [31] J.R. Young, *J. Vac. Sci. Technol.* **10** (1973), p. 212.
- [32] F.W. Lampe, J.L. Franklin and F.H. Field, *J. Am. Chem. Soc.* **79** (1957), p. 6129.
- [33] J.E. Ortega, F.J. Himpsel, D. Li and P.A. Dowben, *Solid State Commun.* **91** (1994), p. 807.
- [34] P.A. Dowben, *Surf. Sci. Rep.* **40** (2000), p. 151.
- [35] N. Sato, K. Seki and H.J. Inokuchi, *J. Chem. Soc. Faraday Trans. II* **77** (1981), p. 1621.
- [36] H. Fukagawa, H. Yamane, T. Kataoka, S. Kera, M. Nakamura, K. Kudo and N. Ueno, *Phys. Rev. B* **73** (2006), p. 245310.
- [37] P.G. Schroeder, C.B. France, J.B. Park and B.A. Parkinson, *J. Phys. Chem. B* **107** (2003), p. 2253.
- [38] J.F. Moulder, W.F. Stickle, P.E. Sobol, K.D. Bomben (Eds.), *Handbook of X-ray Photoelectron Spectroscopy*, Perking-Elmer Corporation, Physical Electronics Division, 1992.
- [39] C. Kunz, E.E. Koch, G.K. Wertheim, H. Hochst, L. Ley, M. Campagna, M. Cardona, P. Steiner, R.A. Pollak, S. Hufner, W.D. Grobman and Y. Baer In: L. Ley and M. Cardona, Editors, *Photoemission In Solids II: Case Studies; Topics in Applied Physics* Vol. 27, Springer-Verlag, Berlin Heidelberg New-York (1979).
- [40] P.A. Dowben, M. Grunze and D. Tomanek, *Phys. Scripta* **T4** (1983), p. 106.
- [41] D. Tomanek, P.A. Dowben and M. Grunze, *Surf. Sci.* **126** (1983), p. 112.
- [42] Jie Xiao, Carolina Ilie, Ning Wu, Keisuke Fukutani and P.A. Dowben, *Surf. Sci.* **603** (2009), p. 513.
- [43] P.A. Dowben, Jaewu Choi, E. Morikawa, Bo Xu, The band structure and orientation of molecular adsorbates on surfaces by angle-resolved electron spectroscopies, in: H.S. Nalwa (Ed.), *Handbook of Thin Films*, vol. 2: Characterization and Spectroscopy of Thin Films, Academic Press, 2002, pp. 61-114 (Chapter 2).
- [44] G. Kaindl, T.-C. Chiang, D.E. Eastman and F.J. Himpsel, *Phys. Rev. Lett.* **45** (1980), p. 1808.
- [45] X.J. Zhou and K.T. Leung, *J. Phys. Chem. B* **110** (2006), p. 9601.
- [46] J.M. Meyers and A.J. Gellman, *Surf. Sci.* **337** (1995), p. 40.
- [47] L. Kilian, A. Hauschild, R. Temirov, S. Soubatch, A. Schöll, A. Bendounan, F. Reinert, T.-L. Lee, F.S. Tautz, M. Sokolowski and E. Umbach, *Phys. Rev. Lett.* **100** (2008), p. 136103.
- [48] P.G. Schroeder, C.B. France, J.B. Park and B.A. Parkinson, *J. Appl. Phys.* **91** (2002), p. 3010.